Chromatographic Study on Liquid-Phase Adsorption on Octadecylsilyl-Silica Gel

Kanji Miyabe
Central Laboratories, Kurita Water Industries Ltd., 7-1, Wakamiya, Morinosato, Atsugi 243-01, Japan

Motoyuki Suzuki
Inst. of Industrial Science, University of Tokyo, 7-22-1, Roppongi, Minato-ku, Tokyo 106, Japan

Adsorption characteristics of reversed-phase liquid chromatography and influence of solvent composition on the characteristics are studied by the chromatographic method and the moment analysis. Adsorption equilibrium constant increases by adding hydrophobic increments into adsorbate molecules. Contributions of fluid-to-particle mass transfer and intraparticle diffusion to mass-transfer resistance in the octadecylsilyl-silica gel (ODS) column are almost equally great. Surface diffusion is dominant for the intraparticle diffusion in ODS. The logarithm of the surface diffusion coefficient linearly increases with an increase in methanol fraction in the range from 40 to 100 vol. %. In liquid-phase adsorption, activation energy of surface diffusion is greater than the isosteric heat of adsorption and both increase when methanol fraction decreases in the range from 40 to 100 vol. %. An empirical correlation based on experimental data proposed estimates surface diffusion coefficients from physical properties of adsorbates.

Introduction

Many kinds of liquid chromatographic techniques are frequently employed for both analytical and preparative separations and reversed-phase mode is the most widely used among them. It is estimated that about 70–80% of analytical separations have been carried out by using a reversed-phase technique. In the field of reversed-phase chromatography, octadecylsilyl silica gel (ODS) is used as a stationary phase in most cases (Bidlingmeyer, 1987; Krstulovic and Brown, 1982; Poole and Poole, 1991; Sander and Wise, 1987). Many kinds of techniques can be used in reversed-phase separation by modifying in mobile-phase conditions and bringing about extensive applications of reversed-phase liquid chromatography. For example, gradient elution makes possible both fine separations between compounds similar in chemical properties and simultaneous separations between ones extremely different in adsorbability (Jandera and Churacek, 1985). The possibility of gradient elution methods results from chemical stability of reversed-phase packing materials and rapid attainment in equilibrium state.

In order to make a rational design of chromatographic processes for separation of mixtures, information on adsorption rate as well as adsorption equilibrium of each component on ODS is essential. Quite a few works have been reported on retention behaviors on the surface of ODS. Effects of several parameters such as solvent composition of mobile phase, chain length of chemically bonded ligand, and properties of adsorbates on the retention behaviors have been extensively studied. Very few works, however, have been carried out so far on diffusion phenomena in ODS particles, in contrast to the extensive studies concerning retention behaviors.

Since chromatographic separation can be effectively controlled by changing mobile-phase conditions, optimization of these conditions plays an important role in establishing a preferable separation. Extensive studies have been carried out on the effect of a solvent and mobile-phase compositions on separation properties such as retention behaviors. A number of experimental results have been reported bringing about different conclusions. In reversed-phase mode, mixed solvents of organic modifiers and water are employed as a mobile phase. A few organic solvents such as methanol, acetonitrile, and tetrahydrofuran are used as an organic modifier. A linear relation is usually observed between the logarithm of capacity factor, k' (or adsorption equilibrium constant, K) and volumetric fraction, ϕ, of an organic solvent in mobile

Correspondence concerning this article should be addressed to K. Miyabe.

phase. Analysis and prediction of chromatographic separations are usually carried out based on the linear relation. Berendsen and de Galan (1980) showed that the linear relation could be observed in the range of k' larger than unity and that the slope of the linear relation was correlated to retention behaviors. Similar results were reported by Schoenmakers et al. (1979). They also suggested that curvature of the relationship between log k' and ϕ observed in the range of k' smaller than unity was dependent on the kind of an organic modifier. Karger et al. (1976) reported that similar relationship was observed when acetonitrile and water mixed solvent was used as a mobile phase and that for methanol and water mixture a linear correlation was obtained irrespective of the value of k'. Hennion et al. (1978) also suggested that a linear relation between log k' and ϕ was obtained regardless of mobile-phase conditions. A linear relation between log k' and ϕ was theoretically interpreted by applying the solvophobic theory. Horvath et al. (1976, 1977, 1978) studied the influence of solvophobic interactions on the retention behaviors of reversed-phase liquid chromatography.

On the other hand, few studies have been made on mass-transfer phenomena in reversed-phase chromatography. We reported earlier the study on liquid-phase adsorption of *p*-tert-octylphenol on the surface of ODS by the chromatographic technique and the moment analysis method (Miyabe and Suzuki, 1992, 1993a). In ODS particles, surface diffusion is dominant for intraparticle diffusion. The surface diffusion coefficient increased with an increase in the amount adsorbed. The positive concentration dependence of the surface diffusion coefficient could be interpreted in terms of diffusion by chemical potential driving force. Energetical uniformity of the surface of ODS was also confirmed from analyses of adsorption equilibrium and thermodynamic parameters. Moreover, we determined adsorption rates and thermodynamic parameters in a gaseous system (Miyabe and Suzuki, 1993b). It was concluded that the contribution of intraparticle diffusion to the overall mass transport resistance in ODS column was dominant and the role of surface diffusion was significant for the intraparticle diffusion.

In liquid-phase adsorption, intraparticle diffusion is influenced by several parameters such as temperature, amount adsorbed, and presence of a solvent. Dependence of intraparticle diffusion on temperature and concentration of an adsorbate has been extensively studied in both gas- and liquid-phase adsorption systems. Correlations between intraparticle diffusion coefficient and some physical properties of an adsorbate have also studied. Few articles, however, have been published on the effect of a solvent on mass transfer in adsorbent particles. Awum et al. (1988) investigated a liquid-phase adsorption of benzene on a zeolite. As a solvent, *n*-hexane and cyclohexane were employed. Intracrystalline diffusion coefficient of benzene in liquid-phase adsorption scattered around the extrapolation of Arrhenius' plot for a corresponding gaseous system. In reversed-phase liquid chromatography, mobile-phase composition is one of the most dominant factors, which intensively influence separation properties. Effect of solvent composition on mass-transfer rate is also an important subject.

This article is concerned with adsorption characteristics of liquid-phase adsorption with ODS. Effects of the presence of a solvent and solvent compositions on adsorption characteristics were studied. In reversed-phase liquid chromatography, "adsorption" and "partition" have been proposed as retention mechanisms. In this study, mass transfer of solutes from a bulk phase to a surface of ODS are interpreted as an adsorption phenomena in a broad sense. Chromatographic measurements were made by using several organics as an adsorbate in the temperature range from 288 to 308 K. Not only adsorption equilibrium but also mass-transport rates and thermodynamic properties of adsorption phenomena on ODS were determined from the moment analysis of pulse response curves observed experimentally. An attempt was made to estimate surface diffusion coefficient in ODS from properties of adsorbates.

Moment Analysis

Chromatographic peaks leaving from a column were analyzed by the method of moment (Suzuki, 1973, 1990). Adsorption equilibrium constant, K, was determined from first moment analysis. Second moment analysis provided information about all the mass-transfer steps involved in adsorption processes. Intraparticle diffusion coefficient was determined by subtracting the effects of axial dispersion and fluid-to-particle mass transfer. The details of the method were described in the previous article (Miyabe and Suzuki, 1992).

The first absolute moment and the second central moment of a chromatographic peak are:

$$\mu_1 = \int Ce(t)tdt \Big/ \int Ce(t)dt = (z/u_0)\delta_0 \tag{1}$$

$$\mu'_2 = \int Ce(t)(t-\mu_1)^2 dt \Big/ \int Ce(t)dt = (2z/u_0)(\delta_{ax} + \delta_f + \delta_d) \tag{2}$$

$$\delta_0 = \epsilon + (1-\epsilon)(\epsilon_p + \rho_p K) \tag{3}$$

$$\delta_{ax} = (Ez/u_0^2)\delta_0^2 \tag{4}$$

$$\delta_f = (1-\epsilon)(R/3k_f)(\epsilon_p + \rho_p K)^2 \tag{5}$$

$$\delta_d = (1-\epsilon)(R^2/15De)(\epsilon_p + \rho_p K)^2 \tag{6}$$

The first moment was analyzed by Eq. 7 derived from Eq. 1:

$$(\mu_1 - t_0)/(1-\epsilon) = (z/u_0)\rho_p K \tag{7}$$

where

$$t_0 = (z/u_0)[\epsilon + (1-\epsilon)\epsilon_p] \tag{8}$$

The value of t_0 is an elution time of an inert pulse. According to Eq. 7, a linear relationship should be observed between $(\mu_1 - t_0)/(1-\epsilon)$ and z/u_0. Adsorption equilibrium constant, K, was calculated from the slope of the linear plot.

For analysis of the second moment, a parameter H was calculated:

$$H = (\mu_2'/\mu_1^2)(z/2u_0) = (Ez/u_0^2) + H_0 \quad (9)$$

$$H_0 = \delta_d/\delta_0^2 \quad (10)$$

Intraparticle diffusion coefficient was determined from the intercept of the linear plots between H vs. $1/u_0$. The value of δ_f was calculated from Eq. 5 and its contribution to the second moment was subtracted. Fluid-to-particle mass-transfer coefficient, k_f, was estimated by the equation of Wilson-Geankiplis.

$$Sh = (1.09/\epsilon)Sc^{1/3}Re_p^{1/3} \quad (11)$$

Molecular diffusivity, Dm, of an adsorbate in methanol-water mixture was estimated by the Wilke-Chang equation.

$$Dm = 7.4\times10^{-8}(a_2M_2)^{1/2}T/\eta_2V_1^{0.6} \quad (12)$$

The contribution of adsorption rate at an adsorption site to the second moment was assumed to be negligibly small. The plot of H vs. $1/u_0$ provides axial dispersion coefficient, Ez, and intraparticle diffusivity, De, from the slope and the intercept, respectively. Surface diffusion coefficient, Ds, was calculated by correcting the contribution of pore diffusion to the intraparticle diffusion:

$$De = Dp + \rho_p KDs \quad (13)$$

Pore diffusivity, Dp, was estimated from molecular diffusivity, porosity, and tortuosity of pores according to the following equation:

$$Dp = \left(\epsilon_p/k^2\right)Dm \quad (14)$$

Tortuosity factor was determined from chromatographic experiments with inert pulses.

When an elution peak can be approximated by the normal distribution curve, the first and the second moments can be determined from the position and the width of the peak, respectively. The experimental first moment, $\mu_{1\text{exp}}$, includes the effects of the volume, Ve, of the pipes between an injection port and a column and that between a column and a detector. The correction of the extra-column volume was made for $\mu_{1\text{exp}}$ as follows:

$$\mu_1 = \mu_{1\text{exp}} - Ve/v \quad (15)$$

The second moment was calculated from a peak width at half height, w, by the equation:

$$\mu_2' = w^2/5.54 \quad (16)$$

The contribution of the pipes to the second moment was measured by the chromatographic method without a column and was corrected. The effect of the first and the second moments of a pulse introduced at the inlet of a column was neglected because the pulse size was extremely small.

Table 1. Properties of ODS Column and Experimental Conditions

Avg. particle dia., d_p (μm)	45
Particle dens., ρ_p (g/cm^3)	0.86
True dens. (g/cm^3)	1.59 (100, 80), 1.60 (60), 1.63 (40, 20), 1.70 (0)
Pore vol. (cm^3/g)	0.53 (100, 80, 60), 0.55 (40, 20), 0.57 (0)
Porosity, ϵ_p	0.46 (100, 80, 60), 0.47 (40, 20), 0.49 (0)
Carbon content (wt. %)	17.1
Mass of ads. (g)	2.1
Column size (mm)	6 ID × 150
Void fraction, ϵ	0.43
Peclet no.	1.0
Tortuosity factor, k^2	4.5
Column temp. (K)	288 ~ 308
Mobile phase	Methanol/water: 100/0 ~ 0/100 (vol.)
Superf. vel., u_o (cm/s)	0.06 ~ 0.12

( ): Volumetric ratio of methanol in methanol/water mobile phase.

Experimental Studies

Apparatus

A high performance liquid chromatograph equipment (LC-6A, Shimadzu) was employed. A small volume of sample solutions was introduced into a fluid flow by use of a sample injector. A column was kept at a constant temperature in a thermostated water bath. The concentration of the sample in effluent was monitored by an ultraviolet or a refractive index detectors.

Column and reagents

The properties of the ODS column (YMC) used in this study are shown in Table 1. The size of the column was 6 mm ID and 150 mm in length. Methanol/water mixtures ranging in concentration of methanol from 0 to 100 vol. % were used as a mobile phase. Pore volume and porosity of ODS particles slightly increased with an increase in methanol fraction in mobile phase. As a sample material, several organics such as *n*-alkanes, *n*-alcohols, benzene derivatives, *p*-*n*-alkylphenols, and aromatic hydrocarbons were used. Sodium nitrate, uracil, and methanol were used as an inert substance to determine a void volume of the ODS column.

Procedure

Experimental conditions are also shown in Table 1. Pulse response experiments were carried out at zero surface coverage with varying temperatures and flow rates of the carrier solvent. Small concentration perturbation pulses were introduced into the carrier flow. Measurements of chromatographic peaks were made in the temperature range from 288 to 308 K. The volumetric flow rate of the carrier solvent was varied in the range from 0.017 to 0.033 cm^3/s. This corresponded to the range of superficial velocity from 0.059 to 0.118 cm/s. Chromatographic peaks observed were analyzed by the method of moment.

Results and Discussion

First moment analysis

Figure 1 shows the typical plots of $(\mu_1 - t_0)/(1-\epsilon)$ vs. z/u_0

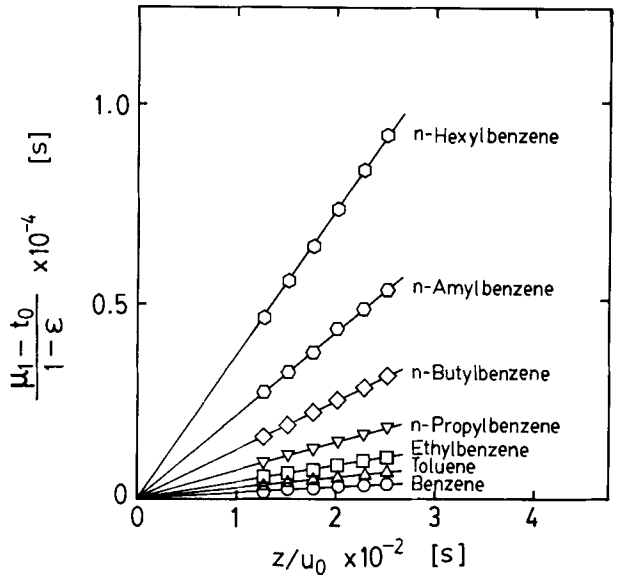

Figure 1. First moment plot of *n*-alkylbenzene derivatives at 298 K.

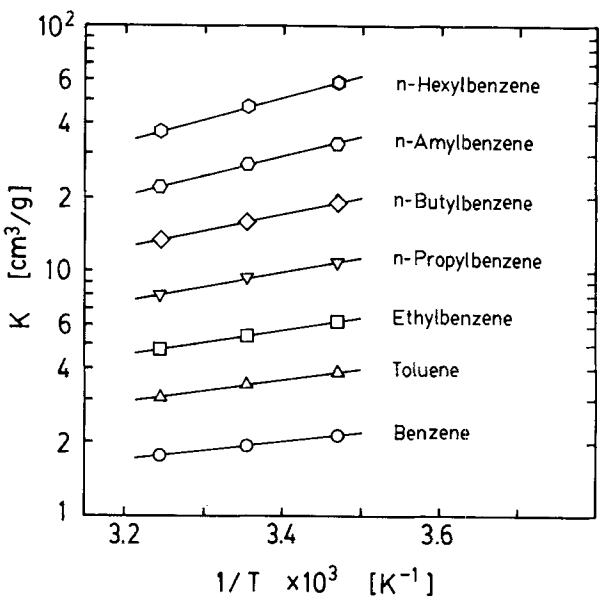

Figure 2. van't Hoff's plot of adsorption equilibrium constants.

for *n*-alkylbenzenes at 298 K. Methanol/water mixture (70/30 by vol.) was used as a mobile phase. Straight lines of different slopes through the origin were observed. The slope increased with an increase in carbon number of *n*-alkyl chain. Adsorption equilibrium constants were calculated from the slope of the linear plots for each adsorbate at various temperatures.

Isosteric heat of adsorption, Q_{st}, was determined by the van't Hoff equation:

$$d \ln K/d(1/T) = -Q_{st}/R_g \qquad (17)$$

According to Eq. 17, K was plotted against $1/T$ for various adsorbates in Figure 2. Resulting values of Q_{st} listed in Table 2 are of the same order of magnitude compared with the other previously reported experimental results (Colin et al., 1978; Colin and Guiochon, 1977, 1978; Horvath and Melander, 1977; Issaq and Jaroniec, 1989; Knox and Vasvari, 1973; Majors and Hopper, 1974; Unger, 1979). The increment in isosteric heat of adsorption resulting from introduction of one methylene group to adsorbate molecules was about 2 kJ/mol.

The logarithm of K_0 indicates entropy change arising from the adsorption of each adsorbate. The adsorption process is accompanied by reduction of entropy in each adsorption system. The magnitude of the entropy reduction for a large molecule was larger than that for a small one.

Figure 3 shows correlation of isosteric heat of adsorption with methanol concentration, ϕ, in mobile phase. The isosteric heat of adsorption increased with a decrease in methanol fraction. Colin et al. (1978) reported similar results for a reversed-phase liquid chromatographic system, in which acetonitrile/water mixture was used as a mobile phase. Oppositely isosteric heat of adsorption decreased in the range of methanol fraction less than 40 vol. %, and a maximum was observed. The presence of the maximum of Q_{st} at $\phi = 40$ vol. % has not been interpreted rigorously. However, the phenomena appear to be related to physical nature of alkyl chains on the surface of ODS. In the range of methanol composition from 40 to 100 vol. %, it may be preferable to adsorb on the surface of ODS rather than dissolve in a bulk phase, as methanol composition decreases in a mobile phase. On the other hand, physical properties of alkyl chains are also changed with mobile-phase conditions. As water content increases in mobile phase, alkyl chains must associate with each other and make collapsed stationary phases. Moreover, alkyl chains interact more and their mobility must be restricted. Adsorption of adsorbates on such collapsed stationary phases may be energetically unstable. So isosteric heat of adsorption might show the maximum at $\phi = 40$ vol. %.

Second moment analysis

Figure 4 shows the typical plots of H vs. $1/u_0$ for *n*-alkylbenzenes at 298 K. Linear relations were observed between H and $1/u_0$. Axial dispersion coefficient was determined from the slope of the linear plots. Peclet number of the ODS column used in this study was calculated to be about 1.0.

Second moment analysis provided information about all the mass-transfer steps involved in adsorption processes. According to the moment analysis of a chromatographic peak, second moment is represented as a sum of contributions of each transfer step in a column. The contributions of each step to the second moment are compared for each adsorbate. Typical data between upper and lower temperature limits were listed in Table 3. For almost all the experiments, the contribution of axial dispersion was found to be ranging from 20 to 30%. The contributions of fluid-to-particle mass-transfer and intraparticle diffusion were of same order of magnitude and change in a same direction with respect to temperature for

Table 2. Experimental Results

Key	Adsorbate	Qst (kJ/mol)	K_g (cm^3/g)	E_s (kJ/mol)	Ds_0 (cm^2/s)
○	Benzene	6.7	1.4×10^{-1}	19.4	7.0×10^{-3}
△	Toluene	8.7	1.1×10^{-1}	20.5	8.7×10^{-3}
□	Ethylbenzene	9.7	1.2×10^{-1}	22.0	1.4×10^{-2}
▽	*n*-Propylbenzene	11.4	9.8×10^{-2}	22.6	1.4×10^{-2}
◇	*n*-Butylbenzene	13.0	8.8×10^{-2}	25.7	4.0×10^{-2}
⬡	*n*-Amylbenzene	15.2	6.2×10^{-2}	26.3	4.3×10^{-2}
⬠	*n*-Hexylbenzene	17.5	4.1×10^{-2}	28.3	8.0×10^{-2}
▨	*p*-Xylene	10.3	9.9×10^{-2}	23.4	2.5×10^{-2}
●	Phenol	8.3	1.9×10^{-2}	16.9	2.2×10^{-3}
▲	*p*-Cresol	8.5	2.9×10^{-2}	16.8	1.7×10^{-3}
■	*p*-Ethylphenol	10.0	2.5×10^{-2}	18.9	3.2×10^{-3}
▼	*p*-*n*-Propylphenol	11.4	2.5×10^{-2}	20.8	5.2×10^{-3}
◆	*p*-*n*-Butylphenol	13.2	2.1×10^{-2}	21.9	6.6×10^{-3}
⬡	*p*-*n*-Hexylphenol	16.7	1.5×10^{-2}	23.4	7.7×10^{-3}
◒	*n*-Hexanol	9.0	4.6×10^{-2}	16.4	1.3×10^{-3}
△	*n*-Heptanol	10.8	3.8×10^{-2}	21.8	9.0×10^{-3}
◧	*n*-Octanol	12.9	2.7×10^{-2}	22.3	8.8×10^{-3}
▽	*n*-Decanol	17.0	1.5×10^{-2}	23.1	7.1×10^{-3}
▽	*n*-Pentane	11.8	9.1×10^{-2}	—	—
◒	*n*-Hexane	12.6	1.1×10^{-1}	—	—
△	*n*-Heptane	14.8	8.0×10^{-2}	—	—
◧	*n*-Octane	17.2	5.1×10^{-2}	—	—
⬡	Cyclohexanol	7.1	5.6×10^{-2}	16.1	1.3×10^{-3}
⬡	Cyclohexane	10.4	1.7×10^{-1}	22.2	8.9×10^{-3}
⊕	Biphenyl	12.3	6.4×10^{-2}	21.9	9.0×10^{-3}
◇	Naphthalene	10.1	8.9×10^{-2}	20.1	4.8×10^{-3}
◇	1-Naphthol	12.2	1.2×10^{-2}	21.7	8.1×10^{-3}
◇	2-Naphthol	11.9	1.2×10^{-2}	20.2	4.6×10^{-3}
⬡	Binaphthyl	17.1	4.4×10^{-2}	30.0	8.4×10^{-2}
□	Anthracene	15.7	2.9×10^{-2}	27.1	5.5×10^{-2}
▽	Nitrobenzene	8.3	4.2×10^{-2}	18.6	6.0×10^{-3}
△	Chlorobenzene	8.1	1.3×10^{-1}	22.6	2.0×10^{-2}
◪	Aniline	7.8	2.1×10^{-2}	20.2	9.5×10^{-3}
◒	Acetophenone	6.0	7.7×10^{-2}	23.5	3.6×10^{-2}
◧	Methylacetophenone	7.8	6.3×10^{-2}	20.4	8.5×10^{-3}
◇	Ethylacetophenone	8.3	8.5×10^{-2}	23.3	2.1×10^{-2}
◒	Methylbenzoate	7.1	9.4×10^{-2}	25.4	5.9×10^{-2}
◧	Ethylbenzoate	8.5	8.4×10^{-2}	23.4	2.2×10^{-2}
◇	*n*-Propylbenzoate	9.7	8.7×10^{-2}	26.7	6.7×10^{-2}

each adsorbate. However, the contribution of fluid-to-particle mass transfer increased as adsorption equilibrium constant increased at each temperature. On the contrary, the contribution of intraparticle diffusion decreased with an increase in adsorption equilibrium constant. The direction of the change in the both contributions was opposite. The contribution of intraparticle diffusion was larger than that of fluid-to-particle mass transfer under the conditions that adsorption equilibrium constant was relatively small.

The contributions of pore and surface diffusions to an intraparticle diffusion were compared with each other. As shown in Table 4, intraparticle diffusion coefficients were a few times or about one or two orders of magnitude larger than pore diffusivities. The contribution of surface diffusion to overall mass transfer in ODS particles was found to be as much as 75–95%. Surface diffusion coefficients were of the order of 10^{-7}–10^{-6} cm^2/s. It is concluded that surface diffusion is dominant for intraparticle diffusion in ODS particles.

Figure 5 shows the correlation of surface diffusion coefficient with methanol composition in mobile phase. The value of *Ds* increased with an increase in methanol fraction irrespective of temperature, and nearly linear relations were observed between logarithm of *Ds* and methanol composition. On the contrary, adsorption equilibrium constants decreased linearly as methanol composition increased. It is concluded that *Ds* seems to be inversely proportional to *K* in the range of methanol concentration from 40 to 100 vol. %.

Activation energy of surface diffusion, *Es*, at zero surface coverage was calculated from the Arrhenius equation:

$$d \ln Ds/d(1/T) = -Es/R_g \tag{18}$$

Typical plots for *n*-alkylbenzenes measured by using 70 vol. % methanol are illustrated in Figure 6.

Figure 7 shows a comparison of Arrhenius' plots in both gas- and liquid-phase adsorption systems. Experimental data could be plotted on an almost identical line for each adsorbate. As listed in the article (Miyabe and Suzuki, 1994), the values of activation energy of surface diffusion were almost equal in both adsorption systems. Similar study was carried out by Awum et al. (1988), who investigated a liquid-phase adsorption of benzene on a zeolite. As a solvent, *n*-

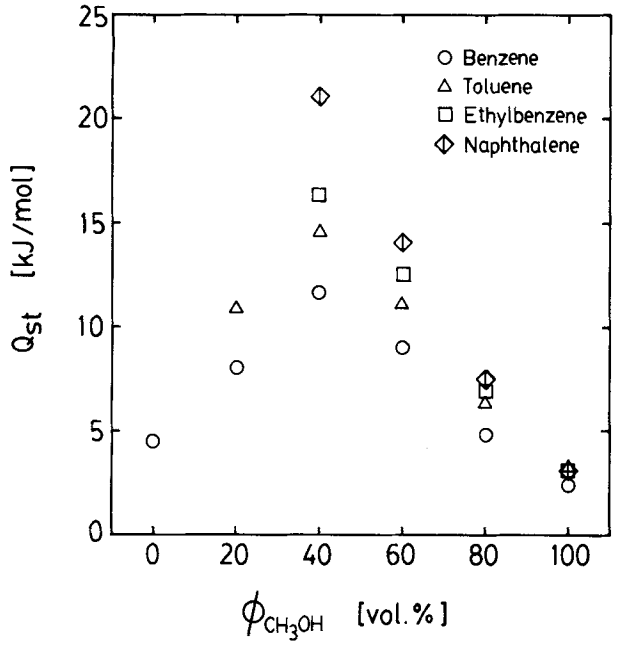

Figure 3. Relationship between isosteric heat of adsorption and methanol composition of the mobile phase.

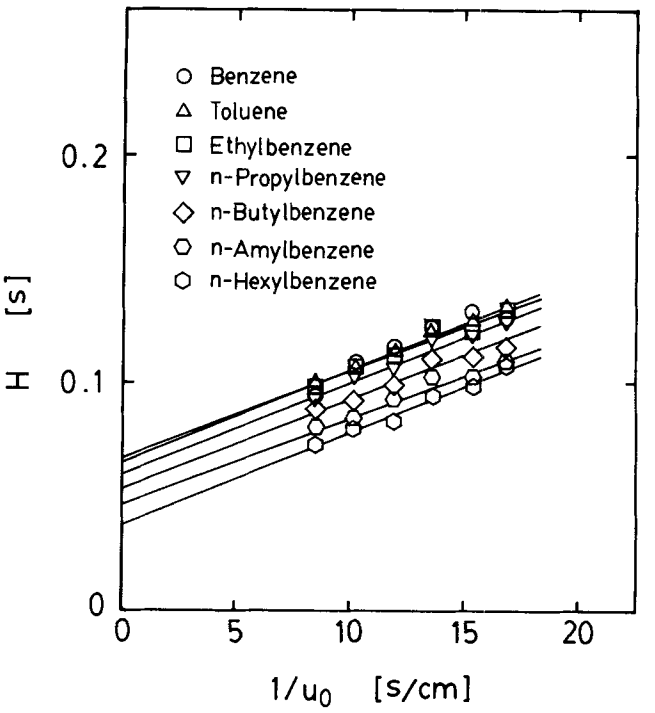

Figure 4. Second moment plot of *n*-alkylbenzene derivatives at 298 K.

hexane and cyclohexane were employed. Intracrystalline diffusion coefficient of benzene in liquid-phase adsorption scattered around the extrapolation of Arrhenius' plot for a corresponding gaseous system. Analysis of experimental data in both gas- and liquid-phase systems may provide information about migration mechanism of adsorbate molecules in reversed-phase chromatography.

Correlations of activation energy of surface diffusion with mobile-phase composition are illustrated in Figure 8. The value of *Es* increased as methanol fraction in mobile phase decreased in the range from 40 to 100 vol. %.

An attempt was made to correlate surface diffusion coefficients on ODS with properties of adsorbates. As a first approximation, it was assumed that the surface migration could

Table 3. Comparison of the Contributions of Axial Dispersion, External Film and Intraparticle Diffusional Resistance

	Temp. (K)	$\mu_1/(z/u_0)$	$\mu'_2/(2z/u_0)$ (s)	δ_{ax} (%)	δ_f (%)	δ_d (%)
Benzene	288	1.8	0.50	20.9	32.3	46.8
	298	1.7	0.37	25.8	30.3	44.2
	308	1.6	0.29	29.3	28.8	41.9
Toluene	288	2.7	1.2	20.8	40.1	39.2
	298	2.5	0.85	23.5	37.7	38.8
	308	2.3	0.61	28.0	35.7	36.3
Ethylbenzene	288	3.9	2.7	20.1	46.8	33.1
	298	3.5	1.8	23.9	44.3	31.8
	308	3.2	1.3	27.7	41.8	30.6
n-Propylbenzene	288	6.3	6.8	19.2	54.2	26.6
	298	5.5	4.4	22.8	51.6	25.6
	308	4.8	2.9	26.2	48.4	25.5
n-Butylbenzene	288	10.6	18.6	17.9	61.5	20.5
	298	9.0	11.7	21.1	58.4	20.5
	308	7.6	7.2	24.3	56.3	19.4
n-Amylbenzene	288	18.1	52.4	15.3	69.1	15.6
	298	14.8	31.1	20.9	64.0	15.1
	308	12.2	18.3	24.0	61.1	14.9
n-Hexylbenzene	288	31.4	156.2	16.3	72.6	11.1
	298	24.9	85.4	19.6	69.1	11.2
	308	19.8	49.0	22.7	66.3	11.0

Table 4. Comparison of the Contributions of Pore and Surface Diffusion

	Temp. (K)	De (cm^2/s)	Dp (cm^2/s)	De/Dp	Ds (cm^2/s)
Benzene	288	4.7×10^{-6}	6.2×10^{-7}	7.6	2.1×10^{-6}
	298	5.7×10^{-6}	8.5×10^{-7}	6.7	2.7×10^{-6}
	308	6.9×10^{-6}	1.1×10^{-6}	6.3	3.6×10^{-6}
Toluene	288	6.5×10^{-6}	5.5×10^{-7}	11.7	1.7×10^{-6}
	298	7.5×10^{-6}	7.5×10^{-7}	10.1	2.2×10^{-6}
	308	9.1×10^{-6}	9.8×10^{-7}	9.4	2.9×10^{-6}
Ethylbenzene	288	8.3×10^{-6}	5.0×10^{-7}	16.8	1.4×10^{-6}
	298	1.0×10^{-5}	6.7×10^{-7}	14.9	1.9×10^{-6}
	308	1.2×10^{-5}	8.8×10^{-7}	13.5	2.5×10^{-6}
n-Propylbenzene	288	1.1×10^{-5}	4.5×10^{-7}	25.0	1.1×10^{-6}
	298	1.4×10^{-5}	6.2×10^{-7}	22.3	1.6×10^{-6}
	308	1.6×10^{-5}	8.1×10^{-7}	19.3	2.0×10^{-6}
n-Butylbenzene	288	1.6×10^{-5}	4.2×10^{-7}	37.6	9.0×10^{-7}
	298	1.8×10^{-5}	5.7×10^{-7}	32.3	1.2×10^{-6}
	308	2.2×10^{-5}	7.5×10^{-7}	30.1	1.8×10^{-6}
n-Amylbenzene	288	2.2×10^{-5}	3.9×10^{-7}	57.0	7.3×10^{-7}
	298	2.6×10^{-5}	5.3×10^{-7}	49.1	1.0×10^{-6}
	308	3.0×10^{-5}	7.0×10^{-7}	43.7	1.5×10^{-6}
n-Hexylbenzene	288	3.2×10^{-5}	3.7×10^{-7}	85.7	5.9×10^{-7}
	298	3.7×10^{-5}	5.0×10^{-7}	72.9	8.6×10^{-7}
	308	4.3×10^{-5}	6.6×10^{-7}	65.0	1.3×10^{-6}

be regarded as a tracer diffusion of an adsorbate molecule in *n*-octadecane. An empirical correlation was presented for the prediction of a tracer diffusivity in binary systems involving long-chain hydrocarbons (Chen and Chen, 1985):

$$10^9 D_{12}\eta_2/TV_{b2}^{2/3} = 11.96/V_{b1}^{1/3} - 0.8796 \qquad (19)$$

According to Eq. 19, surface diffusion coefficients were plotted against $V_{b1}^{-1/3}$ in Figure 9. Tracer diffusivities calculated by Eq. 19 were also illustrated by a dashed line in Figure 9. The values estimated were greater than the experimental data, and the difference between the experimental and calculated values may stem from several factors. For instance, the influence of the tortuosity factor of the surface of ODS particles on the surface diffusion should be considered. The mobility of *n*-octadecylsilyl ligands seems to be restricted in comparison with liquid-like state of *n*-octadecane because one end of the alkyl chain is chemically bonded on the surface of silica gel. The properties of the bonded ligands may be influenced by solvation with the mobile phase. An empirical linear relationship was obtained:

$$Ds = 1.1\times10^{-8}\exp(26.1V_b^{-1/3}) \qquad (20)$$

Because molar volume of an adsorbate at normal boiling point, V_b, can be determined from experimental or calculation methods, Eq. 20 is available in practice to estimate surface diffusion coefficients on ODS particles.

As shown in Table 2, activation energy of surface diffusion was found to be larger than isosteric heat of adsorption in liquid-phase adsorption. Similar experimental results have been reported for surface diffusion phenomena in liquid-phase adsorption systems (Awum et al., 1988; Ching et al., 1989; Ma et al., 1988; Miyabe and Suzuki, 1992, 1993a). These conditions suggest the following unreasonable situation, that is, it is energetically advantageous for adsorbed molecules to desorb from a surface to a bulk phase rather than migrate on the surface denying the presence of surface diffusion phenomena. Analysis of experimental data was attempted to elucidate thermodynamical properties of surface diffusion on ODS.

Suzuki and Kawazoe (1975) studied liquid-phase adsorption of volatile organics from aqueous solution to activated carbon and determined surface diffusion coefficients with batch adsorption method. A linear relation was confirmed between surface diffusion coefficients and the ratio of the boiling point of the adsorbates to adsorption temperature. A surface diffusion coefficient in activated carbon can be estimated by the linear relationship. Suzuki and Kawazoe suggested that the ratio of activation energy of surface diffusion to isosteric heat of adsorption was about 0.5 by analyzing the slope of the linear plot and providing a physical interpretation to a preexponential factor.

Surface diffusion coefficients on ODS were similarly plotted against the ratio of the boiling point of adsorbates to adsorption temperature in Figure 10. The value of boiling point of a polar substance was estimated from that of a corresponding nonpolar homologue, because only the hydrophobic part of an adsorbate molecule should contribute retention phenomena on ODS. Experimental data scattered around straight lines represent the following empirical correlations:

$$Ds = 4.3\times10^{-5}\exp(-2.3T_b/T)\text{—}n\text{-alkylbenzenes} \qquad (21)$$

$$Ds = 5.4\times10^{-5}\exp(-2.6T_b/T)\text{—}n\text{-alkylphenols} \qquad (22)$$

$$Ds = 4.1\times10^{-5}\exp(-2.7T_b/T)\text{—}n\text{-alcohols} \qquad (23)$$

The above equations are corresponding to the conventional Arrhenius form. For example, activation energy, Es, in Eq. 23 can be expressed as follows:

$$Es = 2.7R_gT_b \qquad (24)$$

On the other hand, heat of vaporization is related to T_b according to Trouton's rule:

$$\Delta H_v = 88T_b \qquad (25)$$

The ratio of isosteric heat of adsorption to heat of vaporization, α, was found to range from 1.0 to 1.4 (Miyabe and Suzuki, 1993b). Isosteric heat of adsorption can also be related to T_b:

$$Q_{st} = 88\alpha T_b \qquad (26)$$

By comparing Eq. 24 to Eq. 26, it is suggested that Es is about 0.25 times of Q_{st}. This result is consistent with the ratio of Es/Q_{st} experimentally determined in gas-phase adsorption systems with ODS (Miyabe and Suzuki, 1993b). By analyzing the surface diffusion coefficient, it was also concluded that the value of Es was smaller than Q_{st} in the liquid-phase adsorption system.

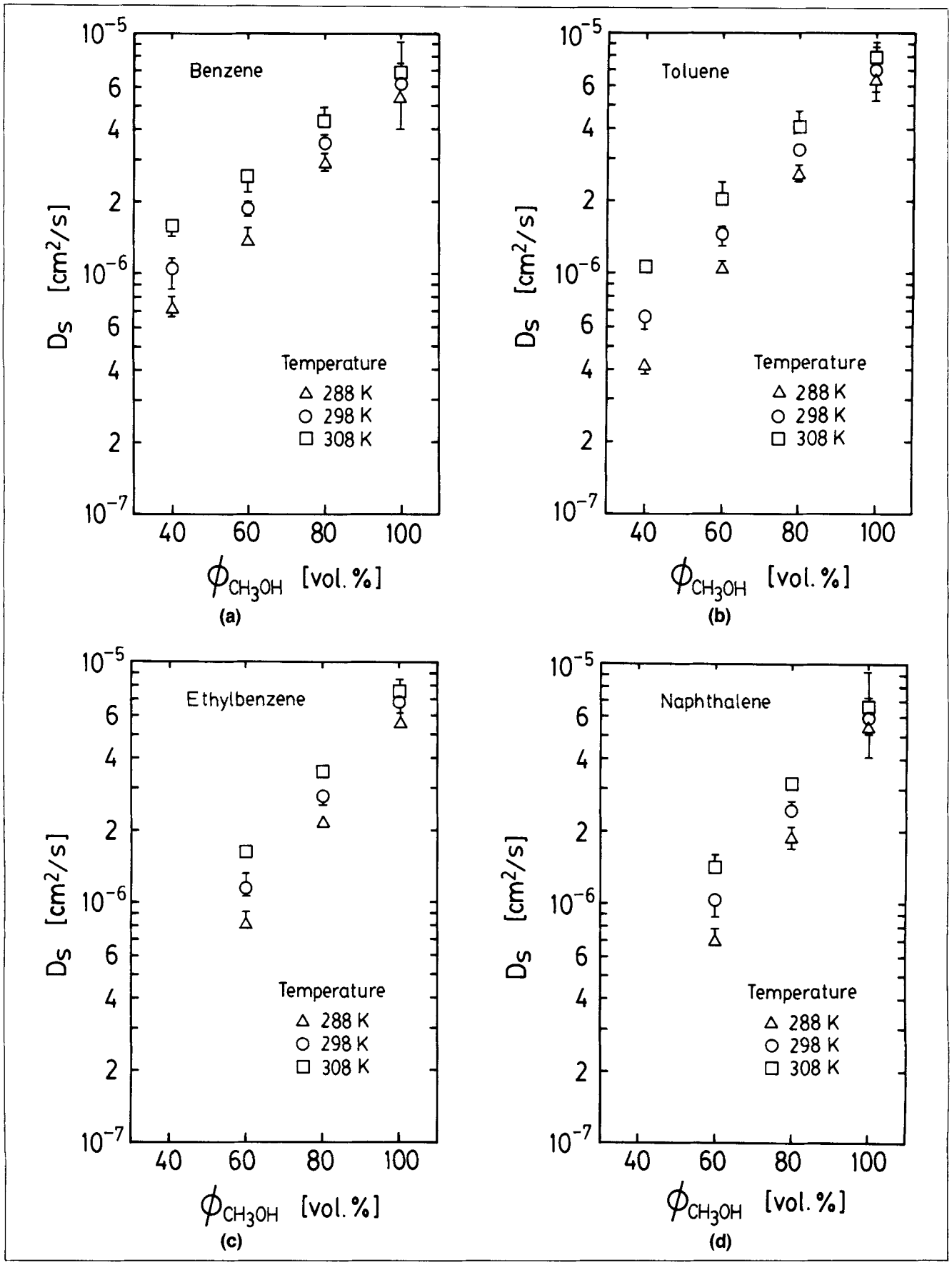

Figure 5. Surface diffusion coefficient as a function of the composition of methanol in the mobile phase.

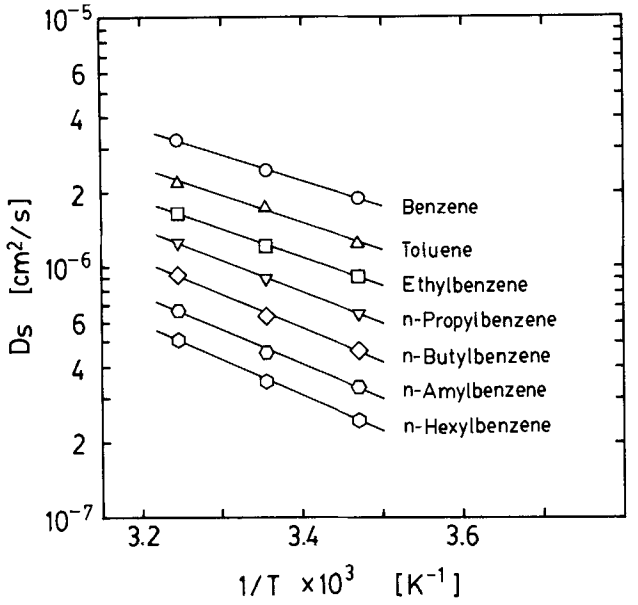

Figure 6. Arrhenius' plots of surface diffusion coefficients.

A different linear relationship seems to be drawn for polyaromatic hydrocarbons. A more detailed study is necessary to clarify the migration mechanism of adsorbate molecule on the surface of ODS. Since there is some scattering in data illustrated in Figure 10, accuracy of the estimation of surface diffusion coefficient may be insufficient. However, it was made possible to estimate the order of surface diffusion coefficient in ODS particles from physical properties of adsorbates.

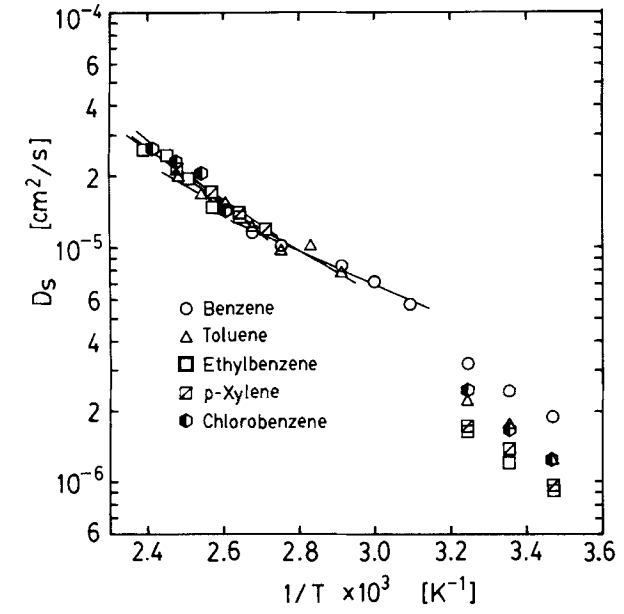

Figure 7. Arrhenius' plots of surface diffusion coefficients in both gas- and liquid-phase adsorption systems.

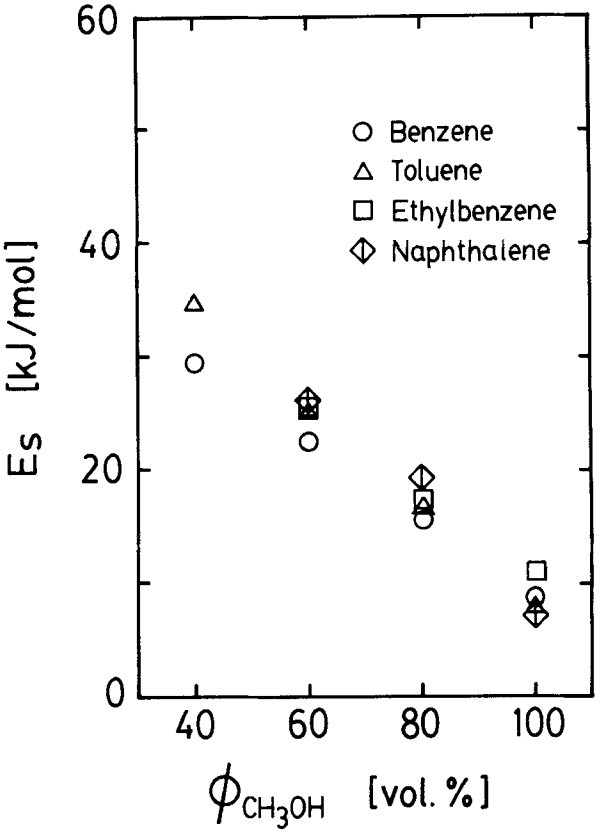

Figure 8. Relationship between activation energy of surface diffusion and methanol composition of the mobile phase.

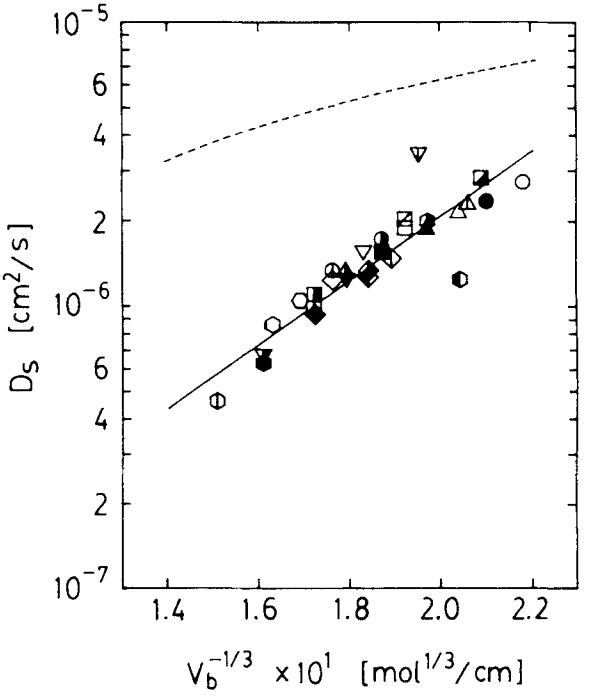

Figure 9. Surface diffusion coefficient against $V_b^{-1/3}$.

V_b is the molecular volume at boiling point (cm³/mol); keys refer to Table 2.

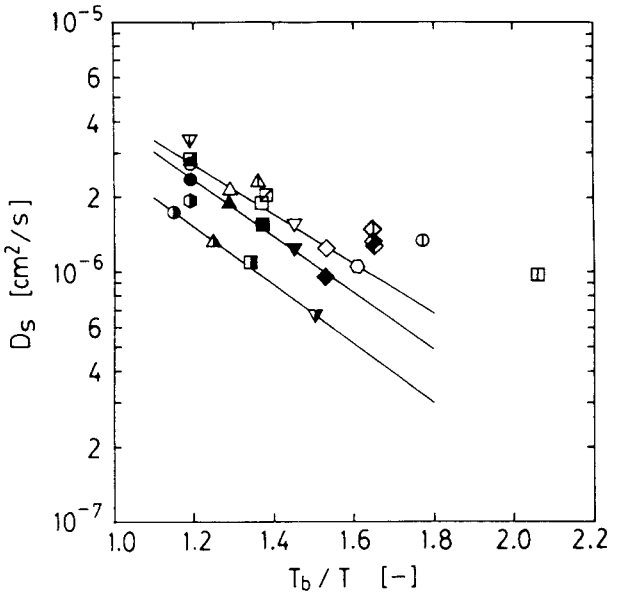

Figure 10. Surface diffusion coefficient against T_b/T.

T_b is the boiling point of adsorbate (K); T is the adsorption temperature (K); keys refer to Table 2.

Conclusion

Adsorption characteristics of ODS were studied by the chromatographic method and the moment analysis. Several kinds of organics were used as an adsorbate. Adsorption characteristics were correlated with the properties and structure of the adsorbates, and the effect of solvent composition on adsorption characteristics of the reversed-phase liquid chromatographic system was also studied.

Adsorption equilibrium constant was increased by adding a hydrophobic increment such as methylene group and phenyl ring. On the other hand, an introduction of hydroxyl group into an adsorbate molecule decreased adsorption equilibrium constant.

For 70 vol. % methanol, isosteric heat of adsorption was about 6–18 kJ/mol and activation energy of the surface diffusion was about 20–30 kJ/mol. In liquid-phase adsorption, activation energy of surface diffusion was determined to be larger than isosteric heat of adsorption. This result appears to be attributed to the influence of a solvent on the liquid-phase adsorption phenomena.

The contributions of fluid-to-particle mass transfer and intraparticle diffusion to mass-transfer resistance in the ODS column were significant and almost equal. Surface diffusion was dominant for the intraparticle diffusion in ODS. About 75–95% of adsorbed molecules migrated by means of surface diffusion, and the surface diffusion coefficients were of the order of 10^{-7}–10^{-6} cm^2/s when 70 vol. % methanol was used as a mobile phase.

By assuming that the surface diffusion on ODS could be regarded as a tracer diffusion of an adsorbate molecule in *n*-octadecane, an empirical correlation based on experimental data was proposed to estimate surface diffusion coefficients with a boiling point or molecular volume of an adsorbate at a boiling point.

Analysis of surface diffusion coefficients provided the conclusion that the ratio of Es to Q_{st} ranged from about 0.2 to 0.25 even in liquid-phase adsorption, and the figure was in agreement with the results in gaseous systems.

The logarithm of the surface diffusion coefficient increased linearly with an increase in methanol fraction in the range from 40 to 100 vol. %. Isosteric heat of adsorption increased with a decrease in methanol fraction, however oppositely decreased in the range of methanol composition lower than 40 vol. %. A maximum was observed at about 40 vol. %. Activation energy of surface diffusion also increased as methanol fraction decreased in the range from 40 to 100 vol. %.

Notation

A = surface area, cm^2/mol
d_p = particle diameter, μm
D = diffusivity, cm^2/s
De = intraparticle diffusion coefficient, cm^2/s
Dp = pore diffusivity, cm^2/s
Ds = surface diffusion coefficient, cm^2/s
Ds_0 = frequency factor, cm^2/s
Es = activation energy of surface diffusion, kJ/mol
Ez = axial dispersion coefficient, cm^2/s
H = defined in Eq. 2
k^2 = tortuosity factor
K = adsorption equilibrium constant, cm^3/g
K_0 = adsorption equilibrium constant at $1/T = 0$, cm^3/g
Q_{st} = isosteric heat of adsorption, kJ/mol
R = particle radius, μm
R_g = gas constant
t = time, s
T = temperature, K
T_b = boiling point, K
u_0 = superficial velocity, cm/s
V_b = molecular volume at normal boiling point, cm^3/mol
V_e = elution volume, cm^3
z = longitudinal position in bed, cm

Greek letters

δ_0 = defined by Eq. 3
δ_{ax} = defined by Eq. 4
δ_d = defined by Eq. 6
δ_f = defined by Eq. 5
ϵ = void fraction in bed
ϵ_p = porosity
η = viscosity, Pa·s
μ_1 = first moment, s
μ'_2 = second moment, s^2
ρ_p = particle density, g/cm^3
ϕ = volumetric fraction of an organic modifier in a mobile phase, %

Subscripts

1 = solute
2 = solvent

Literature Cited

Awum, F., S. Narayan, and D. Ruthven, "Measurement of Intracrystalline Diffusivities in NaX Zeolite by Liquid Chromatography," *Ind. Eng. Chem. Res.*, **27**, 1510 (1988).

Berendsen, G. E., and L. de Galan, "Role of the Chain Length of Chemically Bonded Phases and the Retention Mechanism in Reversed-Phase Liquid Chromatography," *J. Chromatog.*, **196**, 21 (1980).

Bidlingmeyer, B. A., *Preparative Liquid Chromatography*, Elsevier, Amsterdam, p. 203 (1987).

Chen, H. C., and S. H. Chen, "Corresponding-Stats Correlation of Tracer Diffusion in Liquids," *Ind. Eng. Chem. Fundam.*, **24**, 183 (1985).
Ching, C. B., K. Hidajat, and M. S. Uddin, "Evaluation of Equilibrium and Kinetic Parameters of Smaller Molecular Size Amino Acids on KX Zeolite Crystals via Liquid Chromatographic Techniques," *Sep. Sci. Technol.*, **24**, 581 (1989).
Colin, H., J. C. Diez-Masa, G. Guiochon, T. Czajkowska, and I. Miedziak, "The Role of the Temperature in Reversed-Phase High-Performance Liquid Chromatography Using Pyrocarbon-Containing Adsorbents," *J. Chromatog.*, **167**, 41 (1978).
Colin, H., and G. Guiochon, "Introduction to Reversed-Phase High-Performance Liquid Chromatography," *J. Chromatog.*, **141**, 289 (1977).
Colin, H., and G. Guiochon, "Comparison of Some Packings for Reversed-Phase High-Performance Liquid-Solid Chromatography," *J. Chromatog.*, **158**, 183 (1978).
Hennion, M. C., C. Picard, and M. Caude, "Influence of the Number and Length of Alkyl Chains on the Chromatographic Properties of Hydrocarbonaceous Bonded Phases," *J. Chromatog.*, **166**, 21 (1978).
Horvath, C., and W. Melander, "Liquid Chromatography with Hydrocarbonaceous Bonded Phases; Theory and Practice of Reversed-Phase Chromatography," *J. Chromatog. Sci.*, **15**, 393 (1977).
Horvath, C., and W. Melander, "Reversed-Phase Chromatography and the Hydrophobic Effect," *Amer. Lab.*, **10**, 17 (1978).
Horvath, C., W. Melander, and I. Molnar, "Solvophobic Interactions in Liquid Chromatography with Nonpolar Stationary Phases," *J. Chromatog.*, **125**, 129 (1976).
Issaq, H. J., and M. Jaroniec, "Enthalpy and Entropy Effects for Homologous Solutes in HPLC with Alkyl Chain Bonded Phases," *J. Liquid Chromatog.*, **12**, 2067 (1989).
Jandera, P., and J. Churacek, *Gradient Elution in Column Liquid Chromatography, Theory and Practice*, Chap. 4, Elsevier, Amsterdam (1985).
Karger, B. L., J. R. Gant, A. Hartkopf, and P. H. Weiner, "Hydrophobic Effects in Reversed-Phase Liquid Chromatography," *J. Chromatog.*, **128**, 65 (1976).
Knox, J. H., and G. Vasvari, "The Performance of Packings in High-Speed Liquid Chromatography: III. Chemically Bonded Pellicular Materials," *J. Chromatog.*, **83**, 181 (1973).
Krstulovic, A. M., and P. R. Brown, *Reversed-Phase Liquid Chromatography*, Chap. 10, Wiley, New York (1982).
Ma, Y. H., Y. S. Lin, and H. L. Fleming, "Adsorption and Diffusion of Polar and Non-polar Liquids in Aluminas by HPLC," *AIChE Symp. Ser.*, **84**(264), 1 (1988).
Majors, R. E., and M. J. Hopper, "Studies of Siloxane Phases Bonded to Silica Gel for Use in High Performance Liquid Chromatography," *J. Chromatog. Sci.*, **12**, 767 (1974).
Miyabe, K., and M. Suzuki, "Chromatography of Liquid-Phase Adsorption on Octadecylsilyl-Silica Gel," *AIChE J.*, **38**, 901 (1992).
Miyabe, K., and M. Suzuki, "Chromatographic Study of Liquid Phase Adsorption of p-Tert-Octylphenol on Octadecylsilyl-Silica Gel," *Proc. Int. Conf. on Fund. of Adsorp.*, Kodansha, Tokyo, p. 437 (1993a).
Miyabe, K., and M. Suzuki, "Adsorption Characteristics of Octadecylsilyl-Silica Gel in Gaseous Systems," *AIChE J.*, **39**, 1791 (1993b).
Miyabe, K., and M. Suzuki, "Solvent Effect on Adsorption Phenomena in Reversed-Phase Liquid Chromatography," *AIChE J.*, **41**, 536 (1995).
Poole, C. F., and S. K. Poole, *Chromatography Today*, Chap. 4, Elsevier, Amsterdam (1991).
Sander, L. C., and S. A. Wise, "Recent Advances in Bonded Phases for Liquid Chromatography," *CRC Crit. Rev. Anal. Chemistry*, **18**, 299 (1987).
Schoenmakers, P. J., H. A. H. Billiet, and L. de Galan, "Influence of Organic Modifiers on the Retention Behavior in Reversed-Phase Liquid Chromatography and its Consequences for Gradient Elution," *J. Chromatog.*, **185**, 179 (1979).
Suzuki, M., "Notes on Determining the Moments of the Impulse Response of the Basic Transformed Equations," *J. Chem. Eng. Japan*, **6**, 540 (1973).
Suzuki, M., *Adsorption Engineering*, Chap. 6, Kodansha/Elsevier, Tokyo/Amsterdam (1990).
Suzuki, M., and K. Kawazoe, "Effective Surface Diffusion Coefficients of Volatile Organics on Activated Carbon during Adsorption from Aqueous Solution," *J. Chem. Eng. Japan*, **8**, 379 (1975).
Unger, K. K., *Porous Silica*, Elsevier, Amsterdam, p. 122 (1979).

Manuscript received Oct. 4, 1993, and revision received Mar. 28, 1994.